



# ICPRL: Acquiring Physical Intuition from Interactive Control

Xinrun Xu<sup>1,2</sup>, Pi Bu<sup>3</sup>, Ye Wang<sup>4</sup>, Börje F. Karlsson<sup>5</sup>, Shuo Zhang<sup>1</sup>, Ziming Wang<sup>3</sup>, Tengtao Song<sup>3</sup>, Qi Zhu<sup>3</sup>, Jun Song<sup>3,\*</sup>, Zhiming Ding<sup>1,\*</sup>, Bo Zheng<sup>3</sup>

<sup>1</sup>Institute of Software, Chinese Academy of Science,

<sup>2</sup>University of Chinese Academy of Sciences,

<sup>3</sup>Taobao & Tmall Group of Alibaba,

<sup>4</sup>Renmin University of China, <sup>5</sup>Informatics Department, PUC-Rio

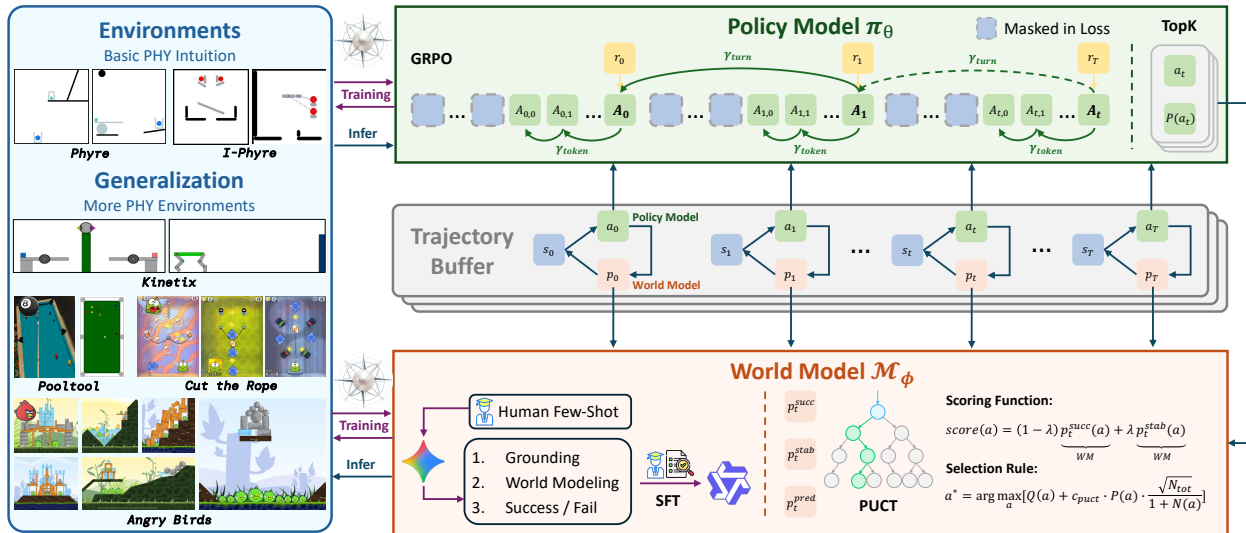


Figure 1: Overview of the ICPRL Framework, which decouples policy learning from world modeling for robust in-context planning. **Training Stage:** We separately train a **Policy Model** ( $\pi_\theta$ ) to generate context-aware actions and a **World Model** ( $\mathcal{M}_\phi$ ) to predict physical outcomes. **Inference Stage:**  $\pi_\theta$  proposes candidate actions, which  $\mathcal{M}_\phi$  evaluates by acting as an *in-context physical simulator*. These evaluations guide a PUCT search to select the optimal action, enabling effective zero-shot planning.

## Abstract

VLMs excel at static perception but falter in interactive reasoning in dynamic physical environments, which demands planning and adaptation to dynamic outcomes. Existing physical reasoning methods often depend on abstract symbolic inputs or lack the ability to learn and adapt from direct, pixel-based visual interaction in novel scenarios. We introduce ICPRL<sup>a</sup> (In-Context Physical Reinforcement Learning), a framework inspired by In-Context Reinforcement Learning (ICRL) that empowers

\*Corresponding Authors.

VLMs to acquire physical intuition and adapt their policies in-context. Our approach trains a vision-grounded policy model via Group Relative Policy Optimization (GRPO) over diverse multi-episode interaction histories. This enables the agent to adapt strategies by conditioning on past trial-and-error sequences, without requiring any weight updates. This adaptive policy works in concert with a separately trained world model that provides explicit physical reasoning by predicting the results of potential actions. At inference, the policy proposes candidate actions, while the world model predicts outcomes to guide a root-node PUCT search to select the most promising action. Evaluated on the diverse physics-based puzzle-solving tasks in the DeepPHY benchmark, ICPRL demonstrates significant improvements across both its: **I.** policy-only, and **II.** world-model-augmented stages. Notably, these gains are retained in unseen physical environments, demonstrating that our framework facilitates genuine in-context acquisition of the environment’s physical dynamics from interactive experience.

<sup>a</sup>Pronounced *IC-Pearl*.

## 1 Introduction

Despite impressive perception, Vision-Language Models (VLMs) struggle with interactive physical reasoning that requires acting, observing consequences, and revising plans. Existing benchmarks largely test static understanding, leaving a gap in closed-loop, physics-grounded competence [1, 2]. Prior work either distills policy improvement from symbolic histories, scales meta-RL [3] with test-time weight updates, or focuses on state-based off-policy in-context RL [4]; however, none directly equips VLMs to learn physics from raw pixels through interaction, to adapt to new tasks in a zero-shot setting [5].

We introduce **ICPRL** (In-Context Physical Reinforcement Learning, an ICRL [6]-inspired VLM framework that enables in-context policy adaptation for interactive physical reasoning. Our approach reinterprets the concept of distilling a policy improvement operator. Instead of training a model to *imitate* the learning trajectory of a separate RL algorithm, our vision-grounded policy model ( $\pi_\theta$ ) directly becomes the subject of policy improvement. We train this VLM using GRPO [7] over a vast collection of diverse, multi-episode interaction histories. This process teaches the model *how* to adjust its strategy based on historical context, including previous successes and failures. Consequently, the ability to adapt to new unseen task instances is not an emergent phenomenon at test time, but rather a robust capability learned and encoded into the model’s weights during training. At inference,  $\pi_\theta$  leverages this ability to improve its performance purely by conditioning on recent interaction history within its forward pass, requiring no further gradient updates. Crucially, we augment this adaptive policy with an independently trained **world model** ( $\mathcal{M}_\phi$ ), which acquires and provides explicit physical intuition by predicting action outcomes and dynamics. This world model serves as a powerful in-context planning component, guiding the policy’s exploration and enabling the agent to discover task-specific physics and refine its plans more efficiently [8, 9].

This two-component architecture is illustrated in Figure 2. Our ICPRL agent (**Right**) consists of: (1) an adaptive **Policy Model** that learns to improve from its interaction history, and (2) an independently trained

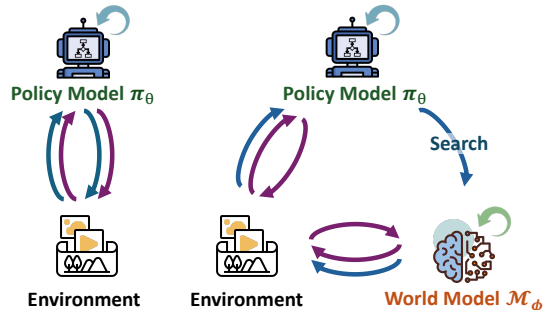


Figure 2: The ICPRL framework integrates world model and adaptive policy.

**World Model** that provides physical intuition. Training interactions for our models are denoted by **purple arrows**. At inference time (**blue arrows**), the policy performs an in-context **Search** over plans simulated by the world model, enabling more efficient reasoning. This approach stands in contrast to conventional agents (**Left**), which train a policy to react directly to environmental feedback without an explicit planning module.

We evaluate ICPRL on DeepPHY [10], a physical benchmark suite spanning single-shot placement to multi-step control, with standardized annotated observations and structured action spaces that preserve physics while enabling reliable VLM control [11]. On the complex multi-step *I-PHYRE* task, our full model achieves a 93.3% success rate. More critically, ICPRL shows remarkable generalization to unseen environments; *e.g.*, on the *Pooltool* task, it achieves a 71.0% success rate, more than doubling the performance of strong baselines like GPT-o3. These gains on tasks the model was never trained on demonstrate that our framework facilitates genuine in-context acquisition of the environment’s physical dynamics from interactive experience.

Building on this evidence, our contributions are twofold: First, we introduce a novel vision-grounded ICRL-inspired framework for VLMs that adapts at test time without weight updates by using interaction histories to infer physics, guided by an explicit world model. Second, we establish state-of-the-art zero-shot performance on diverse interactive physical reasoning tasks, along with analyses on world-model prediction, action discretization, and history length.

## 2 Related Works

### 2.1 In-Context Reinforcement Learning (ICRL)

ICRL represents a paradigm shift in how autonomous agents acquire new skills, moving from slow, gradient-based adaptation to rapid ICL within the forward pass of neural networks. Typically, Algorithm Distillation (AD) [12] distills a policy improvement operator into a Transformer by training on numerous learning histories from a source RL algorithm (*e.g.*, A3C [13]). While methods like AD focus on distilling an external RL algorithm—training a Transformer to *imitate* the learning process itself—our **ICPRL** internalizes this capability directly within the policy model. To circumvent high computational cost, AD<sup>ε</sup> [14] creates synthetic learning histories from a single demonstrator policy by simulating a learning process with a decaying noise curriculum. An alternative approach is memory-based meta-RL [6], in which an agent with persistent memory is trained to improve its strategy over repeated trials on the same task. Such techniques have been extended to LLMs by PAPRIKA [15], fine-tuning on self-generated interaction data using RPO [16]. SCoRe [17] uses on-policy RL to fine-tune an LLM, teaching it a generalizable ICL skill for multi-turn self-correction. ICAL [18] leverages a VLM to autonomously refine noisy interaction data into high-quality examples, enhancing retrieval-augmented ICL planning. ICRL can also leverage Unsupervised Environment Design (UED) and automated curriculum learning to generate diverse and high-quality training tasks. Building on XLand [19], which advanced the training of generalist agents through an open-ended process of dynamic task generation, Adaptive Agent (AdA) [6] introduces an automated curriculum method to navigate the immense XLand 2.0 task space. Prioritized Level Replay (PLR) [20] is a heuristic that focuses training on tasks at the edge of an agent’s competence, and has been theoretically formalized and improved [21–23]. Recent curriculum strategies have advanced from refining task selection at the learning frontier [24] to augmenting the training space with generative models [25], and toward creating truly open-ended domains by evolving the game mechanics themselves [26, 27]. Instead of mimicking an optimization algorithm, our VLM policy is trained via GRPO [7] on multi-episode histories to learn *how to execute* a policy improvement step in-context. By observing diverse histories of trial and error, the VLM learns to condition its future actions on past outcomes, effectively embedding an adaptive, in-context learning skill into its own parameters. This is achieved through gradient-based optimization over multi-episode histories, enabling the VLM to perform in-context adaptation at inference time.

### 2.2 Physical Reasoning in VLMs

Physical reasoning serves as the foundation for world model construction [2, 11] and embodied intelligence tasks [28–30]. However, most evaluations of LLMs & VLMs focus on static problem-solving benchmarks. These evaluations—often large-scale QA tasks on object properties [1, 31] or text-based physics exams

[8, 9, 32]—assess primarily agents’ ability to recall scientific knowledge or infer logical outcomes from fixed contexts. While useful for evaluating declarative knowledge, these approaches largely bypass the challenges of real-time visual perception and continuous interaction in dynamic environments. Another line of research investigates physical reasoning in simulated environments but often abstracts away perceptual grounding by relying on symbolic inputs. Common approaches either provide agents with pre-processed symbolic inputs, such as object property matrices [33–35], or enable interaction with simulators through code generation [36]. While effective for isolating specific planning tasks, these methods limit generalizability by bypassing raw sensory data understanding. Digital game agents [37, 38] have also been used to explore VLM capabilities in modeling realistic dynamics, but while these delve into understanding raw observations, they only require shallow understanding of common sense physics. Our work addresses these limitations by focusing on interactive physical reasoning, where agents must plan and execute a sequence of actions within a physical simulator, guided by learned intuition. Unlike approaches that employ world models for candidate filtering [39] or rely on pre-trained reasoning capabilities [40], ICPRL trains the policy to internalize an improvement operator via GRPO, enabling genuine test-time adaptation through a bi-level optimization process where the world model guides a lookahead search. We adopt DeepPHY [10] as benchmark, covering 6 diverse dynamic physical environments, to evaluate agents’ interactive physical reasoning directly from visual inputs in dynamic environments.

### 3 ICPRL

We consider a family of physical simulators  $\{\mathcal{E}_m\}_{m=1}^M$ . At each decision point we observe  $s_t \in \mathcal{S}$ , choose an action  $a_t \in \mathcal{A}$ , and the simulator returns an updated observation and a task reward or success indicator. Our ICPRL framework comprises distinct training and inference stages, as shown in Figure 1: **Training (two stages)**: We foster **in-context adaptive capabilities** within a VLM **policy model**  $\pi_\theta$  through online GRPO [7] on diverse multi-episode interaction histories. Concurrently, a separate **world model**  $\mathcal{M}_\phi$  is trained offline to acquire robust physical intuition by predicting environment dynamics and outcomes. **Inference**: These two models work in concert.  $\pi_\theta$  proposes contextually informed actions, and  $\mathcal{M}_\phi$ , acting as an **in-context physical simulator**, provides crucial outcome predictions to guide a lightweight **root-node PUCT** [41] search. This separation keeps policy  $\pi_\theta$  learning stable and simulator-grounded, while enabling rapid context-sensitive adaptation and refined planning at test time without further weight updates.

#### 3.1 Mathematical Definitions

In this section, we provide the formal definitions for the components used in the ICPRL framework to ensure reproducibility and clarity.

We formalize the interactive physical reasoning task as a Partially Observable Markov Decision Process (POMDP) augmented with interaction history.

- **State Space ( $\mathcal{S}$ )**: The underlying physical state of the simulator (*e.g.*, positions, velocities, friction coefficients).
- **Observation Space ( $\mathcal{O}$ )**: The visual rendering of the state  $o_t \in \mathcal{O}$ , which may include annotated overlays (as detailed in Section 4.1 & DeepPHY [10]).
- **Action Space ( $\mathcal{A}$ )**: The set of executable commands. While  $\mathcal{A}$  in physics simulators is often continuous, we discretize it into text tokens for VLM processing. For example, in Angry Birds, continuous angles  $\theta \in [0, 90]$  are discretized into integer bins.
- **Success Criteria ( $r_{GT}$ )**: A binary reward signal returned by the environment at the end of an episode.  $r_{GT} = 1$  denotes success;  $r_{GT} = 0$  denotes failure.
- **Trajectory ( $\tau$ )**: A sequence recording a single attempt’s interaction:  $\tau = (o, a, r_{GT})$ .
- **Interaction History ( $H$ )**: A collection of past failure trajectories within the same problem instance:  $H_k = (\tau_1, \tau_2, \dots, \tau_{k-1})$ .

- **Policy Mapping:** The policy  $\pi_\theta(a|o, H)$  maps the current observation and history to a probability distribution over actions.
- **Reference Policy:**  $\pi_{ref}$  is the frozen version of the policy model derived from the Supervised Fine-Tuning (SFT) stage. It serves as the anchor for the KL-divergence penalty in Equation (1), preventing the RL-tuned policy  $\pi_\theta$  from deviating excessively from natural language distribution and maintaining the validity of the output format.

### 3.2 Training Stage: Policy Model $\pi_\theta$

Our policy model  $\pi_\theta$  is a VLM that generates textual outputs in a structured format (detailed in Section 3.4). These outputs are parsed into discrete actions  $a_t \in \mathcal{A}$  by an environment-specific converter, for interaction with simulators across  $M$  environments. The reinforcement signal is derived directly from the task’s native rewards (*e.g.*, success/failure).

While standard RL algorithms can be applied to this setup by treating the agent’s trajectory as a monolithic sequence, this approach often proves suboptimal. It fails to distinguish between agent-generated tokens (reasoning and actions) and environment-provided context, and it applies a uniform temporal discounting that conflates intra-turn and inter-turn credit assignment. To address these limitations, we enhance our training framework by incorporating principles from selective token masking and bi-level advantage estimation [42]. First, we employ **selective token masking** to focus the learning signal; we set  $M_t^{\text{loss}} = 1$  for all tokens generated by the policy  $\pi_\theta$  and  $M_t^{\text{loss}} = 0$  for all other tokens (*e.g.*, those constituting the state observation  $s_k$ ). Second, for multi-turn credit assignment, we adopt a **bi-level advantage estimation** scheme. We set an intra-turn discount  $\gamma_{\text{token}} = 1.0$ , which treats all tokens within a reasoning-action chain as equally contributing to the turn’s outcome. For interactions across turns, we use an inter-turn discount of  $\gamma_{\text{turn}} = 0.9$ , which allows for standard temporal discounting of long-term rewards. These turn-aware mechanisms are used to compute the final token-level advantage estimates,  $A_{i,t}^{\text{GAE}}$ , for our GRPO objective.

We sample a group of tokens  $G$  generated from policy model  $\pi_\theta$ ,  $G = \{o_1, o_2, \dots, o_G\}$ . The importance sampling ratio, denoted as  $r_t(\theta)$ , is defined as the probability ratio between the new and old policies for a given token:  $r_t(\theta) = \pi_\theta(o_{i,t} | q, o_{i,<t}) / \pi_{\theta_{\text{old}}}(o_{i,t} | q, o_{i,<t})$ , where  $o_{i,t}$  is the  $t$ -th token of the  $i$ -th output sample,  $o_{i,<t}$  is the context for generating the token  $o_{i,t}$ . With a frozen reference  $\pi_{\text{ref}}$ , the masked GRPO losses are:

$$\begin{aligned} \mathcal{L}_{\text{GRPO}} = & \frac{1}{G} \sum_{i=1}^G \min \left( r_t(\theta) \cdot \hat{A}_{i,t}, \text{clip}(r_t(\theta), 1 - \varepsilon, 1 + \varepsilon) \cdot \hat{A}_{i,t} \right) \\ & - \beta D_{\text{KL}}(\pi_\theta \| \pi_{\text{ref}}) - \beta D_{\text{KL}}(\pi_\theta(\cdot | q, o_{i,<t}) \| \pi_{\text{ref}}(\cdot | q, o_{i,<t})) \end{aligned} \quad (1)$$

where the relative advantage  $\hat{A}_{i,t}$  for the  $i$ -th response is  $A_i = \frac{r(o_i) - \text{mean}(\{r(o_1), \dots, r(o_G)\})}{\text{std}(\{r(o_1), \dots, r(o_G)\})}$ ,  $q$  is the input prompt given to  $\pi_\theta$ ,  $\varepsilon$  is the PPO clipping hyperparameter, and  $\beta$  is the coefficient for the Kullback-Leibler (KL) divergence penalty.

### 3.3 Training Stage: World Model $\mathcal{M}_\phi$

Given a state-action pair  $(s, a)$ , the **world model**  $\mathcal{M}_\phi$  is trained to return a strictly structured JSON containing a predicted success probability and a natural language prediction.

$$\mathcal{M}_\phi(s, a) \Rightarrow \begin{cases} \hat{p}_{\text{succ}} \in [0, 1], \\ \hat{p}_{\text{pred}} : \text{NL prediction} \end{cases} \quad (2)$$

The predicted success probability  $\hat{p}_{\text{succ}}$  is used directly for planning, while  $\hat{p}_{\text{pred}}$  provides qualitative insights for analysis.

To enhance planning robustness, a stability score,  $\hat{p}_{\text{stab}}$ , is derived from the model’s own predictions. This score is calculated by evaluating the model’s success predictions over a neighborhood of perturbed actions. For an environment-specific action metric  $d_{\mathcal{A}}$  and a radius  $\delta$ , we define the perturbation set as:  $\mathcal{B}_{\delta}(a) = \{a' : d_{\mathcal{A}}(a, a') \leq \delta\}$ . The stability  $\hat{p}_{\text{stab}}$  is the expected model-predicted success rate over actions sampled from this perturbation set. Let  $\hat{p}_{\text{succ}}(s, a')$  denote the success probability predicted by  $\mathcal{M}_{\phi}(s, a')$ . The stability is then defined as:  $\hat{p}_{\text{stab}}(s, a) = \mathbb{E}_{a' \sim D(\mathcal{B}_{\delta}(a))}[\hat{p}_{\text{succ}}(s, a')]$ .

In practice, this expectation is estimated for each sample by querying the model  $\mathcal{M}_{\phi}$  with a small, finite set of “jittered” actions and averaging the resulting  $\hat{p}_{\text{succ}}$  predictions.

---

**Algorithm 1** World Model Dataset Curation.

---

**Require:** Task set  $\mathcal{X}$ ; action space  $\mathcal{A}$ ; simulator  $\text{SIMULATE}(x, a)$  returning video  $\tau$ , action end  $t_{\text{act}}$ , dynamics end  $t_{\text{dyn}}$ , label  $y \in \{0, 1\}$ ; number of frames  $m=5$ ; diversity threshold  $\varepsilon$  (optional).

**Ensure:** WM dataset  $\mathcal{D}_{\text{WM}}$  of tuples  $(x, I_0, I_{\text{ann}}, a, F_{1:m}, y, T)$ .

```

1:  $\mathcal{D}_{\text{WM}} \leftarrow \emptyset$ 
2: for each task  $x \in \mathcal{X}$  do
3:    $I_0 \leftarrow$  initial raw image of  $x$ ;  $I_{\text{ann}} \leftarrow$  initial annotated image of  $x$ 
4:    $S \leftarrow$  all actions in  $\mathcal{A}$  that solve  $x$  ▷ Enumerate via simulation or cache
5:    $k \leftarrow |S|$ 
6:    $F \leftarrow \emptyset$  ▷ Collect  $k$  diverse, failing actions
7:   while  $|F| < k$  do
8:     Sample  $a \sim \mathcal{A} \setminus S$ 
9:     if  $a$  is distinct from  $S \cup F$  (e.g., using distance  $\geq \varepsilon$ ) then
10:       $(y', \_, \_, \_) \leftarrow \text{SIMULATE}(x, a)$ 
11:      if  $y' = 0$  then
12:         $F \leftarrow F \cup \{a\}$ 
13:      end if
14:    end if
15:  end while
16:  for each  $a \in S \cup F$  do
17:     $(\tau, t_{\text{act}}, t_{\text{dyn}}, y) \leftarrow \text{SIMULATE}(x, a)$ 
18:    Uniformly sample  $m$  timestamps in  $(t_{\text{act}}, t_{\text{dyn}}]$  and extract frames  $F_{1:m}$  from  $\tau$ 
19:     $T \leftarrow \text{VLM}(I_0, I_{\text{ann}}, a, F_{1:m}, y)$ 
20:    ▷ Prompt VLM for Grounding & World Modeling text, i.e.,  $p_{\text{pred}}$  ground truth
21:    if human verification passes then
22:       $\mathcal{D}_{\text{WM}} \leftarrow \mathcal{D}_{\text{WM}} \cup \{(x, I_0, I_{\text{ann}}, a, F_{1:m}, y, T)\}$ 
23:    end if
24:  end for
25: end for
26: return  $\mathcal{D}_{\text{WM}}$ 

```

---

To train world model  $\mathcal{M}_{\phi}$ , we first curate a high-quality dataset with a balanced representation of outcomes. This procedure is formalized in Algorithm 1. The data generation process for each initial state  $s$  is as follows:

We first enumerate all possible successful actions from state  $s$ . If  $k$  successful actions are found, we then sample and filter to obtain a corresponding set of  $k$  diverse, failing actions. This ensures a balanced 1:1 ratio of positive to negative examples for each state, preventing model bias. Each successful and failing action is executed in the simulator. We record the entire chain reaction following the action, from its completion until the environment reaches a stable state. From this resulting video sequence, we uniformly sample 5 frames to represent the dynamic evolution of the environment post-action. The collected data—comprising the initial state (raw and annotated images), the action, the five dynamic frames, and the ground-truth success/fail label—is used to generate rich training signals. We employ a large VLM with a few-shot prompting strategy to produce the NLP ground truth for  $\hat{p}_{\text{pred}}$ . The VLM is prompted to generate text describing the objects and their relations in the initial state (**Grounding**), predicting the chain reaction that will occur as a consequence

of the action (**World Modeling**), and providing a **Success or Fail Label**. All automatically generated annotations are then manually inspected and corrected by human reviewers to ensure their accuracy and quality.

With this curated dataset, we train world model  $\mathcal{M}_\phi$ . The training objective combines a regression loss for success prediction and a language modeling loss for the textual output. The total loss  $\mathcal{L}_{\text{WM}}$  is a weighted sum:  $\mathcal{L}_{\text{WM}} = \mathcal{L}_{\text{succ}} + \lambda_{\text{text}}\mathcal{L}_{\text{text}}$ , where  $\mathcal{L}_{\text{succ}} = \text{BCE}(\hat{p}_{\text{succ}}, y)$  is the Binary Cross-Entropy loss between the predicted success probability and the ground-truth label  $y$ , and  $\mathcal{L}_{\text{text}}$  is a standard cross-entropy loss for training the language prediction component.




### 3.4 Inference Stage

At inference time, for each decision point, we employ a root-node search procedure that integrates a learned policy prior with scores from our world model,  $\mathcal{M}_\phi$ . This process, detailed in Algorithm 4.3, unfolds in four stages: candidate generation, scoring, search, and execution.

**Candidate Generation.** First, to form a discrete set of candidate actions  $A = \{a_i\}_{i=1}^K$ , we draw  $S$  samples from our policy network  $\pi_\theta(\cdot | o)$ . Based on these samples, we establish a **frequency prior**  $P(a)$  over the candidate set, defined as  $P(a) = c(a) / \sum_{a' \in A} c(a')$ , where  $c(a)$  is the count of  $a$ .

**Scoring Strategy.** Next, each candidate action  $a \in A$  is evaluated by  $\mathcal{M}_\phi$ . To handle the distinct characteristics of varying physical environments—ranging from stable to chaotic dynamics—we employ two tailored scoring strategies, summarized in Table 1.

Table 1: Calculation Methods of Stability and Uncertainty for PUCT Search.

Environment	Methodology	Action Space	Perturbation / Sampling Details
<b>Strategy 1: Action Space Perturbation for Stability Estimation</b>			
Stability Score: $\hat{p}_{\text{stab}}(a) = \frac{1}{J} \sum_{j=1}^J \mathbb{I}[\mathcal{M}_\phi(o, a'_j) \rightarrow \text{success}]$			
<b>PHYRE</b>	Action Space	$(x, y, r)$ Grid coord. & radius	Perturb $(x, y)$ by $\pm 1$ (4 directions), and $r$ by $\pm 1$ or 0.
<b>I-PHYRE</b>	Perturbation	Sequence of timed events $[(i_k, t_k)]$	Temporal jittering: perturb timestamps $t_k$ with $\pm \Delta t \in \{\pm 0.5\text{s}, \pm 1.0\text{s}\}$ for a subset of events.
 <b>Angry Birds</b>		$(\theta, p)$ Angle & power	Perturb $\theta$ with $\Delta_\theta \in \{-5^\circ, 0^\circ, 5^\circ\}$ and $p$ with $\Delta_p \in \{-0.1, 0, 0.1\}$ .
<b>Strategy 2: Confidence-Based Scoring for Highly Sensitive Environments</b>			
Uncertainty Score (LCB): $\text{score}(a o) = \mu_p - \beta\sigma_p$			
<b>Kinetix</b>	Model Confidence	Varies ( <i>e.g.</i> , timings, forces, positions)	$K = 8$ stochastic forward passes of $\mathcal{M}_\phi(o, a)$ using different temperatures sampled from $[0.1, 1.0]$ . This yields a set of probabilities $\{p^{(j)}\}_{j=1}^K$ .
 <b>Pooltool</b>	(LCB)		
 <b>Cut the Rope</b>			

**Strategy 1: Action Space Perturbation.** For environments with stable physics (*PHYRE*, *I-PHYRE*, *Angry Birds*), we estimate stability by sampling a neighborhood of  $J$  perturbed actions  $\{a'_j\}_{j=1}^J$ . The stability score is the fraction of successful outcomes:  $\hat{p}_{\text{stab}}(s, a) = \frac{1}{J} \sum_{j=1}^J \mathbb{I}[\mathcal{M}_\phi(o, a'_j) \rightarrow \text{success}]$ . Specifically:

- *PHYRE*: We perturb grid coordinates  $(x, y)$  by  $\pm 1$  and radius  $r$  by  $\pm 1$  ( $J = 12$ ).
- *I-PHYRE*: We apply temporal jittering  $\delta \in \{\pm 0.5\text{s}, \pm 1.0\text{s}\}$  to event timestamps, ensuring causal order is preserved.
- *Angry Birds*: We perturb launch angle  $\theta$  by  $\pm 5^\circ$  and power  $p$  by  $\pm 0.1$ .

We combine the mean success prediction  $\mu_p$  and this stability score into:  $\text{score}(a | o) = (1 - \lambda_{\text{PUCT}}) \mu_p(o, a) + \lambda_{\text{PUCT}} \hat{p}_{\text{stab}}(s, a)$ .

---

**Algorithm 2** Inference with Root-Node Search.

---

**Require:** Observation  $o$ ; policy  $\pi_\theta$ ; world model  $\mathcal{M}_\phi$ ; hyperparameters  $S, K, B, \lambda, c_{\text{PUCT}}$ .

**Ensure:** Best action  $a^*$ .

```
1:  $\triangleright$  Stage 1: Candidate Generation and Prior
2:  $A_{\text{samples}} \leftarrow \emptyset$ 
3: for  $i = 1 \rightarrow S$  do
4:   Sample  $a \sim \pi_\theta(\cdot | o)$  and add to  $A_{\text{samples}}$ 
5: end for
6:  $A \leftarrow \text{UNIQUE}(A_{\text{samples}})$ 
7: for each action  $a \in A$  do
8:    $P(a) \leftarrow \text{COUNT}(a, A_{\text{samples}})/S$ 
9: end for
10:  $\triangleright$  Stage 2 & 3: PUCT Search Guided by WM Scores
11:  $N(a) \leftarrow 0, Q(a) \leftarrow 0$  for all  $a \in A$ 
12:  $\text{last\_a} \leftarrow \text{null}, \text{consecutive\_choices} \leftarrow 0$ 
13: for  $t = 1 \rightarrow B$  do
14:    $N_{\text{tot}} \leftarrow \sum_{b \in A} N(b)$ 
15:    $a_t \leftarrow \arg \max_{a \in A} \left[ Q(a) + c_{\text{PUCT}} \cdot P(a) \cdot \frac{\sqrt{N_{\text{tot}}}}{1+N(a)} \right]$ 
16:    $\triangleright$  Early stopping check
17:   if  $a_t = \text{last\_a}$  then  $\text{consecutive\_choices} \leftarrow \text{consecutive\_choices} + 1$ 
18:   else  $\text{consecutive\_choices} \leftarrow 1$ 
19:   end if
20:   if  $\text{consecutive\_choices} \geq 3$  then break
21:   end if
22:    $\text{last\_a} \leftarrow a_t$ 
23:    $\triangleright$  Get WM score by querying K times
24:    $p_{\text{succ\_list}} \leftarrow [], p_{\text{stab\_list}} \leftarrow []$ 
25:   for  $j = 1 \rightarrow K$  do
26:      $\hat{p}_{\text{succ}}^{(j)} \leftarrow \mathcal{M}_\phi(o, a_t)$ 
27:      $\hat{p}_{\text{stab}}^{(j)} \leftarrow \mathbb{E}_{a' \sim D(\mathcal{B}_\delta(a_t))} [\mathcal{M}_\phi(o, a') \cdot \hat{p}_{\text{succ}}^{(j)}]$ 
28:      $\triangleright$  Estimated via jitters
29:     Append  $\hat{p}_{\text{succ}}^{(j)}$  to  $p_{\text{succ\_list}}$ ;  $\hat{p}_{\text{stab}}^{(j)}$  to  $p_{\text{stab\_list}}$ 
30:   end for
31:    $\mu_p \leftarrow \text{MEAN}(p_{\text{succ\_list}}); \mu_s \leftarrow \text{MEAN}(p_{\text{stab\_list}})$ 
32:    $s_t \leftarrow (1 - \lambda)\mu_p + \lambda\mu_s$ 
33:    $\triangleright$  Update search statistics
34:    $Q(a_t) \leftarrow (Q(a_t) \cdot N(a_t) + s_t)/(N(a_t) + 1)$ 
35:    $N(a_t) \leftarrow N(a_t) + 1$ 
36: end for
37:  $\triangleright$  Stage 4: Final Selection
38:  $a^* \leftarrow \arg \max_{a \in A} Q(a)$ 
39: return  $a^*$ 
```

---

*Strategy 2: Model Confidence (LCB).* For environments sensitive to initial conditions (*Kinetix*, *Pooltool*, *Cut the Rope*), we instead estimate the model’s epistemic uncertainty. We perform  $K = 8$  stochastic forward passes with temperatures sampled from  $[0.1, 1.0]$  to obtain success probabilities  $\{p^{(j)}\}_{j=1}^K$ . We then compute a Lower Confidence Bound (LCB) score:  $\text{score}(a|o) = \mu_p - \beta \cdot \sigma_p$ , where  $\mu_p$  and  $\sigma_p$  are the mean and standard deviation of predictions, and  $\beta = 0.2$ . This penalizes uncertain actions in more chaotic domains.

**PUCT Search.** These scores guide a search at the root node. For a planning budget of  $B$  iterations, we select the action  $a_t$  that maximizes the PUCT criterion:

$$a_t = \arg \max_{a \in A} \left[ Q(a) + c_{\text{PUCT}} \cdot P(a) \cdot \frac{\sqrt{\sum_{b \in A} N_{\text{tot}}(b)}}{1 + N(a)} \right] \quad (3)$$

Upon selecting  $a_t$ , its world model score is used to update  $Q(a_t)$  and  $N(a_t)$ . We employ an **early-stopping** mechanism if the budget  $B$  is exhausted, the same action is chosen 3 times consecutively, or a highly successful action ( $\mu_p > 0.8$ ) is found.




**Execution.** Finally, the action  $a^* = \arg \max_a Q(a)$  is executed for a single step.

## 4 Experiments

### 4.1 Experimental Setup

This subsection details the experimental environments, comparison baselines, evaluation metrics, and the implementation details of ICPRL.

#### 4.1.1 Environments & Task Specifications

We adopt DeepPHY [10] as our evaluation platform. This benchmark comprises six diverse and interactive physical simulation environments: *PHYRE* [33], *I-PHYRE* [34], *Kinetix* [35],  *Pooltool* [43],  *Angry Birds*<sup>1</sup>, and  *Cut the Rope*<sup>2</sup>. Encompassing a wide spectrum of physical properties (*e.g.*, gravity, elasticity, collisions), these environments present challenges ranging from single-step planning (*PHYRE*) to complex multi-step sequential control (*Kinetix*, *Cut the Rope*).

To ensure a rigorous interactive evaluation, we formally define the task structure and success metrics below:

#### Formal Definitions.

- **Episode (Task Instance):** An episode refers to the complete problem-solving process for a single specific level or puzzle configuration (*e.g.*, PHYRE template 00002:001). An episode concludes when the agent successfully solves the task or exhausts the maximum allowed attempts.
- **Attempt (Trial):** An episode consists of a sequence of up to  $K$  attempts. At the start of attempt  $k$ , the agent receives the visual observation and the text history of previous failed trajectories  $H_{k-1} = \{\tau_1, \dots, \tau_{k-1}\}$  to perform in-context learning. For PHYRE and I-PHYRE (training environments), the limit is  $K = 10$ . For evaluation environments like Pooltool and Angry Birds, limits are set according to Table 3.
- **Action Horizon (Per Attempt):** This defines the temporal complexity of a single plan within one attempt.
  - *Single-step / In-advance:* The agent outputs a complete static plan (*e.g.*, placing one ball in PHYRE) or a sequence of timed actions (I-PHYRE) at the start. The simulator then executes the physics until stability.

<sup>1</sup><https://apps.apple.com/us/app/rovio-classics-angry-birds/id1596736236>

<sup>2</sup><https://apps.apple.com/cn/app/cut-the-rope/id1024507512>

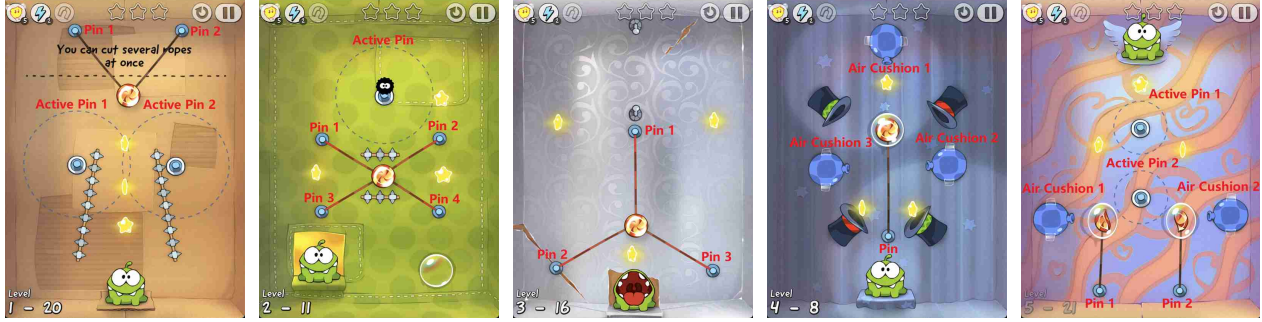


Figure 3: Examples of static element annotation in the *Cut the Rope* game. Key static props—such as Pins, Active Pins, and Air Cushions—are clearly marked with numerical IDs. This method converts pixel-level visual information into grounded tokens, enabling the Agent to accurately identify and manipulate objects.

- *Sequential / On-the-fly*: The agent interacts with the environment in a turn-based manner (e.g., Kinetix, Angry Birds), observing intermediate states between actions.

**Environment Specifications.** We provide a detailed summary of the input modalities, action spaces, and success criteria for all environments in Table 2 and Table 3.

Table 2: Detailed Specifications of DeepPHY Environments (Part I): Input Modalities and Action Spaces.

Environment	Input Modality	Action Space Format
<b>PHYRE</b>	Image + 8×8 Grid Overlay	Discretized Selection: Cell: [1-64], Radius: [1-8]
<b>I-PHYRE</b>	Image + Index IDs	JSON Sequence: [{"time": t, "index": i}, ...]
<b>Kinetix</b>	Image + Motor/Thruster IDs	JSON Vector: [m_1, m_2, ..., t_1, t_2]
<b>Pooltool</b>	2D Top-down View	Discretized Selection: Speed: [Low/Med/High], Strikespot: [Spin]
<b>Angry Birds</b>	Screenshot (Annotated)	Code: [shoot(angle=int, power=float)]
<b>Cut the Rope</b>	Screenshot (Annotated)	Code: [cut_pin(id)], [pop_bubble(id)], etc.

Table 3: Detailed Specifications of DeepPHY Environments (Part II): Horizons and Success Criteria.

Environment	Horizon	Success Criteria ( $r_{GT} = 1$ )
<b>PHYRE</b>	Single-step	Green ball touches Target.
<b>I-PHYRE</b>	Sequence	All Red balls fall into abyss.
<b>Kinetix</b>	Multi-step (Max 16)	Green shape touches Blue, avoids Red.
<b>Pooltool</b>	Multi-step (Max 15)	Pot the 9-ball legally.
<b>Angry Birds</b>	Multi-step (Birds avail.)	All pigs are eliminated.
<b>Cut the Rope</b>	Multi-step	Candy reaches <i>Om Nom</i> 's mouth.

**Implementation Example: Cut the Rope.** To illustrate how continuous gaming environments are adapted for VLM control, we detail the implementation of the *Cut the Rope* task (visualized in Figure 3).

*Visual Input:* The model receives a screenshot where interactive elements are annotated with numerical IDs. For example, a rope anchored to a pin might be labeled “Pin 1”, and a floating bubble containing candy might be labeled “Bubble 2”.

*Action Space:* Instead of continuous gestures, the model outputs structured Python-like function calls within square brackets. The interpreter parses these tokens into game actions. Supported commands include: [cut\_pin(id=3)] to cut a specific rope, [pop\_bubble(id=2)] to release candy, or [sleep(seconds=0.5)] to handle swing dynamics.

### 4.1.2 Evaluation Protocol

To rigorously assess the acquisition of transferable physical intuition, we strictly define our evaluation protocol by partitioning the DeepPHY suite into source and target domains.

We train the Policy Model ( $\pi_\theta$ ) and World Model ( $\mathcal{M}_\phi$ ) exclusively on *PHYRE* and *I-PHYRE*. The models are evaluated on *Kinetix*, *Pooltool*, *Angry Birds*, and *Cut the Rope*. We enforce a strict zero-shot inference setting on the Target Domains. No weight updates, fine-tuning, or parameter calibration are permitted on these environments. The agent must rely solely on its learned physical intuition and in-context adaptation capabilities to solve these unseen tasks.

### 4.1.3 Baselines

We compare ICPRL with leading closed-source and open-source VLMs, as detailed in Table 7. These closed-source models represent the current SOTA in zero-shot physical reasoning. We use the random action agent (*MOCK*) (provided by DeepPHY) as a lower bound on performance.

We evaluate two distinct variants of our own method: i) **ICPRL (Policy Only)**: This variant performs inference using only our policy model,  $\pi_\theta$ , trained with GRPO, without leveraging the world model or PUCT search. This baseline is designed to measure the performance of the adaptive policy itself. And ii) **ICPRL (Full)**: Our complete model, which combines the adaptive policy  $\pi_\theta$  with the PUCT search guided by World Model  $\mathcal{M}_\phi$ , showcasing how both work in tandem.

### 4.1.4 Evaluation Metrics

We employ two core metrics for our evaluation: **Success Rate (S.R.)**, which is the percentage of tasks solved successfully; and **Average Attempts (Avg. Att.)**, the mean number of attempts taken, calculated only on successfully solved tasks. We report Success Rate and Average Attempts over three runs under the different settings.

### 4.1.5 Implementation Details

**Model Architecture:** Both Policy Model  $\pi_\theta$  and World Model  $\mathcal{M}_\phi$  are built and trained based on Qwen2.5-VL-3B/7B-Instruct [44].

**Training:** We conducted training for Policy Model  $\pi_\theta$  and World Model  $\mathcal{M}_\phi$  on the first two environments (*PHYRE* & *I-PHYRE*<sup>3</sup>), and then evaluated their generalization performance on the remaining four. Policy Model  $\pi_\theta$  is trained online using GRPO [7]. For training, we set the actor and critic learning rates to  $1 \times 10^{-6}$  and  $1 \times 10^{-5}$ , respectively. The policy updates are regularized with a KL penalty coefficient ( $\beta$ ) of 0.001. We employ a bi-level advantage estimation with a turn-level discount factor  $\gamma_{\text{turn}} = 0.95$  and a token-level discount  $\gamma_{\text{token}} = 1.0$ . During the online data collection (rollout) phase, actions are sampled using a temperature of 0.7 and top-p nucleus sampling of 0.95. World Model  $\mathcal{M}_\phi$  is trained offline on the curated dataset, with the loss weight for the text component,  $\lambda_{\text{text}}$ , set to 0.2.

**Inference:** The PUCT search is configured with a candidate sample size of  $S = 32$ ,  $K = 8$  world model queries per action, a planning budget of  $B = 32$ , a score mixing weight of  $\lambda_{\text{PUCT}} = 0.25$ , and an exploration coefficient of  $c_{\text{PUCT}} = 1.5$ .

## 4.2 Main Results

The main results, shown in Table 4<sup>4</sup>, provide a comprehensive evaluation of the **ICPRL** framework and its components. Their analysis validates our core hypotheses regarding in-context physical reinforcement learning, the role of world models, and the importance of training paradigms for generalization in complex physical reasoning tasks.

---

<sup>3</sup>Although similarly named, the environments pose distinct challenges: *PHYRE* centers on single-step actions that trigger complex chain reactions, while *I-PHYRE* requires multi-step planning with precise temporal and sequential control.

<sup>4</sup>Unlike the results in the original DeepPHY, we report **S.R.** on the test set for *PHYRE* and *I-PHYRE* environments. The results for all other environments are identical to those in DeepPHY.

Table 4: Overall Performance on DeepPHY. Model naming conventions are detailed in Appendix.

Model Configuration			In-Domain (Training)				Out-of-Distribution (Zero-shot)				
Row Ann.	Policy Model $\pi_\theta$	World Model $\mathcal{M}_\phi$	PHYRE		I-PHYRE		Kinetix	Pooltool		Angry Birds	Cut the Rope
			Att. 1	Att. 10	Att. 1	Att. 10		Att. 1	Att. 15		
# 01.	MOCK	-	1.50%	10.80%	23.33%	53.33%	21.40%	2.33%	48.00%	17.65%	11.36%
<b>Open-Source Models</b>											
# 02.	Qwen-3B	-	0.17%	5.85%	13.33%	16.67%	16.22%	0.00%	50.00%	17.65%	7.95%
# 03.	Qwen-7B	-	0.67%	10.10%	32.42%	32.42%	13.51%	23.50%	26.50%	20.59%	9.09%
# 04.	Qwen-32B	-	0.03%	8.70%	0.17%	5.60%	15.20%	0.00%	14.29%	26.47%	6.82%
# 05.	Qwen-72B	-	2.43%	14.92%	13.33%	43.33%	14.86%	0.00%	18.00%	29.41%	13.64%
# 06.	Qwen-72B	Qwen-72B	1.78%	10.39%	10.00%	36.67%	12.16%	0.00%	14.00%	26.47%	11.50%
<b>Close-Source Models</b>											
# 07.	Claude 4.0 Opus	-	1.73%	10.63%	36.67%	56.67%	23.20%	0.00%	49.00%	32.35%	26.14%
# 08.	Claude 4.0 Opus	Claude 4.0 Opus	1.11%	7.44%	30.00%	50.00%	20.50%	0.00%	42.00%	29.41%	23.86%
# 09.	Gemini-2.5-Pro	-	2.17%	22.07%	20.00%	63.33%	24.10%	36.50%	68.00%	35.29%	22.73%
# 10.	Gemini-2.5-Pro	Gemini-2.5-Pro	2.17%	12.33%	16.67%	53.33%	21.80%	25.00%	60.00%	29.41%	20.45%
# 11.	GPT-o3	-	3.03%	30.77%	30.00%	86.67%	26.89%	0.00%	25.67%	35.29%	18.18%
# 12.	GPT-o3	GPT-o3	0.17%	25.60%	25.00%	76.67%	24.50%	0.00%	22.00%	29.41%	16.50%
<b>Fine-tuned Models</b>											
<b>Qwen2.5-VL-3B-Instruct Fine-tuned Series</b>											
# 13.	Qwen-3B <sup>P</sup> SFT	-	1.33%	25.58%	20.00%	30.00%	13.70%	0.00%	51.00%	23.53%	10.23%
# 14.	Qwen-3B <sup>P</sup> SFT	Qwen-3B <sup>P</sup>	1.52%	28.69%	19.87%	32.45%	13.55%	0.00%	53.67%	26.47%	11.85%
# 15.	Qwen-3B <sup>I</sup> SFT	-	0.33%	9.83%	23.33%	45.56%	9.60%	0.00%	43.00%	20.59%	7.80%
# 16.	Qwen-3B <sup>I</sup> SFT	Qwen-3B <sup>I</sup>	0.74%	11.88%	23.21%	47.34%	9.82%	0.00%	45.33%	23.53%	9.13%
# 17.	Qwen-3B <sup>P&amp;I</sup> SFT	-	10.42%	29.00%	20.00%	50.00%	15.07%	0.00%	57.00%	26.47%	11.60%
# 18.	Qwen-3B <sup>P&amp;I</sup> SFT	Qwen-3B <sup>P&amp;I</sup>	10.70%	33.56%	21.29%	52.91%	15.11%	0.00%	59.67%	32.35%	14.05%
# 19.	Qwen-3B <sup>P</sup> GRPO	-	9.50%	29.03%	13.33%	26.67%	12.33%	0.00%	58.00%	26.47%	11.05%
# 20.	Qwen-3B <sup>P</sup> GRPO	Qwen-3B <sup>P</sup>	9.85%	32.00%	12.78%	28.00%	12.33%	0.00%	61.00%	29.41%	12.98%
# 21.	Qwen-3B <sup>I</sup> GRPO	-	0.17%	9.67%	36.67%	48.89%	8.20%	0.00%	50.00%	20.59%	7.75%
# 22.	Qwen-3B <sup>I</sup> GRPO	Qwen-3B <sup>I</sup>	0.66%	13.48%	37.60%	51.00%	8.07%	0.00%	52.33%	23.53%	9.88%
# 23.	Qwen-3B <sup>P&amp;I</sup> GRPO	-	14.00%	34.50%	36.67%	60.00%	19.18%	0.00%	55.00%	29.41%	12.10%
# 24.	Qwen-3B <sup>P&amp;I</sup> GRPO	Qwen-3B <sup>P&amp;I</sup>	14.11%	39.49%	35.66%	61.99%	19.45%	0.00%	57.33%	35.29%	15.80%
<b>Qwen2.5-VL-7B-Instruct Fine-tuned Series</b>											
# 25.	Qwen-7B <sup>P</sup> SFT	-	3.67%	36.13%	13.33%	19.33%	15.07%	2.00%	66.00%	38.24%	15.35%
# 26.	Qwen-7B <sup>P</sup> SFT	Qwen-7B <sup>P</sup>	3.40%	38.67%	13.57%	22.15%	15.31%	2.00%	67.33%	41.18%	17.50%
# 27.	Qwen-7B <sup>I</sup> SFT	-	0.67%	9.33%	12.22%	50.00%	13.70%	1.00%	64.00%	23.53%	8.21%
# 28.	Qwen-7B <sup>I</sup> SFT	Qwen-7B <sup>I</sup>	0.82%	13.45%	11.34%	51.50%	13.49%	1.00%	66.67%	26.47%	10.36%
# 29.	Qwen-7B <sup>P&amp;I</sup> SFT	-	7.50%	42.67%	20.00%	63.33%	15.07%	2.00%	67.00%	41.18%	16.55%
# 30.	Qwen-7B <sup>P&amp;I</sup> SFT	Qwen-7B <sup>P&amp;I</sup>	7.95%	44.85%	21.41%	65.38%	14.88%	2.00%	69.00%	44.12%	19.33%
# 31.	Qwen-7B <sup>P</sup> GRPO	-	13.00%	40.00%	16.67%	28.89%	13.70%	0.00%	66.00%	41.18%	16.10%
# 32.	Qwen-7B <sup>P</sup> GRPO	Qwen-7B <sup>P</sup>	13.18%	43.66%	15.68%	30.00%	13.91%	0.00%	69.00%	44.12%	18.88%
# 33.	Qwen-7B <sup>I</sup> GRPO	-	0.67%	8.33%	26.67%	86.67%	16.44%	0.00%	60.00%	23.53%	7.95%
# 34.	Qwen-7B <sup>I</sup> GRPO	Qwen-7B <sup>I</sup>	0.67%	13.04%	27.82%	89.31%	16.44%	0.00%	63.00%	26.47%	10.15%
# 35.	Qwen-7B <sup>P&amp;I</sup> GRPO	-	14.63%	43.17%	13.33%	90.00%	19.18%	0.00%	69.00%	45.61%	17.05%
# 36.	Qwen-7B <sup>P&amp;I</sup> GRPO	Qwen-7B <sup>P&amp;I</sup>	14.92%	45.56%	13.12%	93.33%	18.96%	0.00%	71.00%	47.06%	21.20%

Our finetuned methods, including both SFT and GRPO, significantly improve the performance of the utilized base open-source VLM, Qwen2.5-VL. The base models struggle to effectively solve these tasks, which demonstrates that our training pipeline successfully triggers and guides the VLMs to acquire physical intuition. Furthermore, after undergoing the identical fine-tuning process, the 7B models consistently outperform their 3B counterparts, highlighting the benefits of scaling model capacity. The premier configuration, **Qwen-7B<sup>P&I</sup> GRPO** paired with **Qwen-7B<sup>P&I</sup>** (Row #36), consistently achieves state-of-the-art or comparable performance across nearly all tasks. This result validates our central hypothesis: the synergy between an adaptive policy ( $\pi_\theta$ ), trained via GRPO on multi-episode interaction histories, and an independently-trained world model ( $\mathcal{M}_\phi$ ), that guides planning, is critical for mastering complex physical challenges. Notably, this model not only excels in the trained environments (*PHYRE* and *I-PHYRE*) but also exhibits remarkable generalization to entirely unseen tasks in the other four diverse settings, demonstrating the acquisition of robust and transferable physical intuition.

A direct comparison between models trained with SFT (e.g., Row #29) and those trained with GRPO (e.g., Row #35) reveals the clear superiority of the latter. While SFT enables learning from expert trajectories, GRPO’s online policy optimization teaches the agent to dynamically **adapt its strategy in-context** by conditioning on a history of successes and failures. This capability is fundamental to the ICRL paradigm, resulting in a more robust and adaptive policy that is particularly effective in tasks that inherently involve trial-and-error and iterative problem-solving.

The contribution of World Model ( $\mathcal{M}_\phi$ ) is pivotal, transforming the agent from a purely reactive decision-maker into a deliberative planner. Across all finetuned pairs in the table, the full ICPL configuration (Policy +

World Model) consistently outperforms the policy-only variant. This confirms that the world model, acting as an in-context physical simulator, provides crucial foresight. The resulting “propose-verify-select” mechanism, where the policy generates candidate actions and the world model guides a PUCT search to select the most promising one, elevates the agent’s reasoning from simple reaction to improved look-ahead planning. Conversely, employing a generic, non-fine-tuned VLM as a world model (comparing pairs from Rows #5 vs. #6 to #11 vs. #12) degrades performance. This finding, consistent with the original DeepPHY, underscores that general-purpose VLMs currently lack fine-grained interactive physical reasoning capabilities.

Moreover, models trained jointly on both *PHYRE* and *I-PHYRE* (marked as **P&I**) demonstrate superior performance on unseen tasks, when compared to models trained on either environment in isolation (*cf.* Rows #31, #33, and #35). Specifically, the **Qwen-7B<sup>P&I</sup> GRPO** policy (Row #35) outperforms its single-environment counterparts across three unseen testbeds. This supports our hypothesis that exposure to diverse physical dynamics enables the model to internalize a more generalizable “policy-improvement operator,” facilitating the transfer of learned physical intuition to new domains.

In the *Kinetix* environment, however, our models do not exhibit the same magnitude of performance gain as seen in the other environments. We attribute this to its unique nature, which demands precise fine-grained control of sub-object components and their tight interactions. In contrast, the other environments primarily involve reasoning about the holistic behavior and trajectory of whole objects.

### 4.3 Ablation Studies

Our primary SFT models are trained on a dataset of successful solution trajectories from expert models (Gemini-2.5-Pro, GPT-4o, etc., detailed in Appendix), which often include multiple attempts (typically 5–10) before reaching a solution. This strategy is founded on the hypothesis that exposure to this trial-and-error process, even within a supervised framework, enables the model to internalize an iterative problem-solving strategy, aligning with the principles of ICRL.

To validate this hypothesis, we conduct a controlled ablation study detailed in Table 5. We compare our standard SFT models against ablated variants (denoted with a ‘single’ subscript). These ablated models are trained exclusively on a dataset of first-attempt successful trajectories generated via a systematic enumeration process. To ensure the comparison is fair, the number of training samples was kept identical for both SFT methods within the same environment.

Table 5: **Ablation Study:** Performance of Multi-Attempt vs. Single-Attempt Training Trajectories.

(a) <i>PHYRE</i> Benchmark.						(b) <i>I-PHYRE</i> Benchmark.					
Policy Model Only	Avg. Att.	Att. 1	Att. 4	Att. 7	Att. 10	Policy Model Only	Avg. Att.	Att. 1	Att. 4	Att. 7	Att. 10
<i>MOCK</i>	5.00	1.50%	5.87%	8.60%	10.80%	<i>MOCK</i>	3.81	23.33%	43.33%	46.67%	53.33%
<b>Qwen-3B</b>	3.98	0.17%	4.69%	5.67%	5.85%	<b>Qwen-3B</b>	2.87	13.33%	16.67%	16.67%	16.67%
<b>Qwen-3B<sup>single</sup> SFT</b>	2.60	7.63%	17.20%	19.83%	20.97%	<b>Qwen-3B<sup>single</sup> SFT</b>	2.97	33.43%	33.43%	34.54%	34.54%
<b>Qwen-3B<sup>P</sup> SFT</b>	2.89	1.33%	16.58%	20.33%	25.58%	<b>Qwen-3B<sup>I</sup> SFT</b>	3.72	23.33%	30.00%	43.33%	45.56%
<b>Qwen-3B<sup>P</sup> GRPO</b>	3.23	9.50%	25.13%	28.80%	29.03%	<b>Qwen-3B<sup>I</sup> GRPO</b>	3.81	36.67%	43.33%	45.56%	48.89%
<b>Qwen-7B</b>	5.10	0.67%	5.33%	8.17%	10.10%	<b>Qwen-7B</b>	2.20	32.42%	32.42%	32.42%	32.42%
<b>Qwen-7B<sup>single</sup> SFT</b>	2.61	13.17%	21.58%	26.97%	29.14%	<b>Qwen-7B<sup>single</sup> SFT</b>	3.44	35.56%	35.56%	35.56%	35.56%
<b>Qwen-7B<sup>P</sup> SFT</b>	3.74	3.67%	27.33%	34.20%	36.13%	<b>Qwen-7B<sup>I</sup> SFT</b>	3.53	12.22%	46.67%	50.00%	50.00%
<b>Qwen-7B<sup>P</sup> GRPO</b>	5.70	13.00%	33.17%	41.77%	40.00%	<b>Qwen-7B<sup>I</sup> GRPO</b>	4.37	26.67%	43.33%	53.33%	86.67%
<b>Qwen-32B</b>	3.97	0.03%	3.10%	6.93%	8.70%	<b>Qwen-32B</b>	1.40	0.17%	5.60%	5.60%	5.60%
<b>Qwen-72B</b>	4.48	2.43%	9.53%	12.40%	14.92%	<b>Qwen-72B</b>	2.00	13.33%	30.00%	43.33%	43.33%

While the ‘single’ models demonstrate strong initial performance (Att. 1), they often plateau, a behavior particularly pronounced on the *I-PHYRE* benchmark. In contrast, models trained on multi-attempt data exhibit a significantly steeper improvement curve, ultimately achieving superior performance by the final attempts (Att. 10). This confirms that learning from a history of failures and recoveries is crucial for developing a more robust policy. Furthermore, the success rate for our models trained on multi-attempt trajectories consistently and monotonically increases as the interaction history lengthens. A compelling trend is found where the average number of attempts for successful solutions (Avg. Att.) tends to increase in tandem with the model’s capability (*e.g.*, from **SFT** to **GRPO** variants). This suggests that more advanced models are not simply more efficient, but are capable of tackling more complex problems that inherently require a

Table 6: **Ablation Study:** Impact of Dynamic Visual Feedback on World Model Training.

(a) <i>PHYRE</i> Benchmark.				(b) <i>I-PHYRE</i> Benchmark.			
Policy Model	World Model	Att. 1	Att. 10	Policy Model	World Model	Att. 1	Att. 10
Qwen-3B <sup>P</sup> <i>SFT</i>	-	1.33%	25.58%	Qwen-3B <sup>I</sup> <i>SFT</i>	-	23.33%	45.56%
Qwen-3B <sup>P</sup> <i>SFT</i>	Qwen-3B <sup>P</sup> <sub>w/o 5 Frames</sub>	1.40%	27.19%	Qwen-3B <sup>I</sup> <i>SFT</i>	Qwen-3B <sup>I</sup> <sub>w/o 5 Frames</sub>	22.81%	45.04%
Qwen-3B <sup>P</sup> <i>SFT</i>	Qwen-3B <sup>P</sup>	1.52%	28.69%	Qwen-3B <sup>I</sup> <i>SFT</i>	Qwen-3B <sup>I</sup>	23.21%	47.34%
Qwen-3B <sup>P</sup> <i>GRPO</i>	-	9.50%	29.03%	Qwen-3B <sup>I</sup> <i>GRPO</i>	-	36.67%	48.89%
Qwen-3B <sup>P</sup> <i>GRPO</i>	Qwen-3B <sup>P</sup> <sub>w/o 5 Frames</sub>	9.95%	30.20%	Qwen-3B <sup>I</sup> <i>GRPO</i>	Qwen-3B <sup>I</sup> <sub>w/o 5 Frames</sub>	36.97%	47.29%
Qwen-3B <sup>P</sup> <i>GRPO</i>	Qwen-3B <sup>P</sup>	9.85%	32.00%	Qwen-3B <sup>I</sup> <i>GRPO</i>	Qwen-3B <sup>I</sup>	37.60%	51.00%
Qwen-7B <sup>P</sup> <i>SFT</i>	-	3.67%	36.13%	Qwen-7B <sup>I</sup> <i>SFT</i>	-	12.22%	50.00%
Qwen-7B <sup>P</sup> <i>SFT</i>	Qwen-7B <sup>P</sup> <sub>w/o 5 Frames</sub>	3.40%	37.47%	Qwen-7B <sup>I</sup> <i>SFT</i>	Qwen-7B <sup>I</sup> <sub>w/o 5 Frames</sub>	11.34%	50.30%
Qwen-7B <sup>P</sup> <i>SFT</i>	Qwen-7B <sup>P</sup>	3.40%	38.67%	Qwen-7B <sup>I</sup> <i>SFT</i>	Qwen-7B <sup>I</sup>	11.34%	51.50%
Qwen-7B <sup>P</sup> <i>GRPO</i>	-	13.00%	40.00%	Qwen-7B <sup>I</sup> <i>GRPO</i>	-	26.67%	86.67%
Qwen-7B <sup>P</sup> <i>GRPO</i>	Qwen-7B <sup>P</sup> <sub>w/o 5 Frames</sub>	12.68%	41.76%	Qwen-7B <sup>I</sup> <i>GRPO</i>	Qwen-7B <sup>I</sup> <sub>w/o 5 Frames</sub>	27.12%	87.51%
Qwen-7B <sup>P</sup> <i>GRPO</i>	Qwen-7B <sup>P</sup>	13.18%	43.66%	Qwen-7B <sup>I</sup> <i>GRPO</i>	Qwen-7B <sup>I</sup>	27.82%	89.31%

longer iterative process. This provides direct empirical evidence that the models have learned to leverage ICL to interact with the environment and parse physical intuition. Finally, the outstanding performance of the **GRPO** models further underscores the efficacy of our approach.

Table 6 evaluates the importance of providing the World Model with visual information about the dynamic consequences of an action during its training phase. We compare the full model against a variant where the World Model was trained without the five uniformly sampled post-action frames (detailed in Algorithm ). Across both *PHYRE* and *I-PHYRE*, and for all policy model configurations, the full ICPRL framework—which leverages a world model trained with post-action visual frames—consistently outperforms the variant employing an ablated world model (data curated by *w/o 5 Frames*). This performance delta provides strong evidence that incorporating explicit visual feedback of an action’s dynamic consequences is crucial for training an effective world model. Which, in turn, enhances its predictive fidelity, directly translating to more effective guidance for the PUCT search procedure at inference time. Furthermore, it is noteworthy that even the ablated world model generally provides some performance lift over the policy-only baseline, underscoring the fundamental utility of our decoupled two-component architecture for deliberative planning.

## 5 Conclusion

In this work, we introduced **ICPRL** (In-Context Physical Reinforcement Learning), a framework designed to address the limitations of existing VLMs in interactive reasoning within dynamic physical environments. Our framework integrates adaptive policy model with world model that provides explicit physical intuition. Our extensive evaluations on the diverse DeepPHY benchmark demonstrate that ICPRL not only achieves significant performance gains over strong baselines but, crucially, maintains robust generalization, enables genuine in-context acquisition of an environment’s physical dynamics directly from interactive experience.

While ICPRL represents a significant step forward, this work also highlights promising avenues for future research. First, the policy and world models in the current framework are trained independently. Future work could explore synergistic training paradigms where the models are co-trained, allowing data generated by one to inform and enhance the learning process of the other, potentially creating a virtuous cycle of improvement. Second, our analysis revealed that while ICPRL excels at learning overarching physical principles, its performance gains were less pronounced on tasks like in the *Kinetix* environment, which demands high-dexterity, component-level manipulation. This distinction suggests that such fine-grained control problems may constitute a distinct class of challenges, representing another promising direction for future investigation.

## References

- [1] Yi Ru Wang, Jiafei Duan, Dieter Fox, and Siddhartha Srinivasa. Newton: Are large language models capable of physical reasoning?, 2023.
- [2] Niket Agarwal, Arslan Ali, Maciej Bala, Yogesh Balaji, Erik Barker, Tiffany Cai, Prithvijit Chattopadhyay, Yongxin Chen, Yin Cui, Yifan Ding, et al. Cosmos world foundation model platform for physical AI. [arXiv preprint arXiv:2501.03575](#), 2025.
- [3] Yan Duan, John Schulman, Xi Chen, Peter L Bartlett, Ilya Sutskever, and Pieter Abbeel. RL<sup>2</sup>: Fast reinforcement learning via slow reinforcement learning. [arXiv preprint arXiv:1611.02779](#), 2016.
- [4] Jake Grigsby, Linxi Fan, and Yuke Zhu. Amago: Scalable in-context reinforcement learning for adaptive agents. [arXiv preprint arXiv:2310.09971](#), 2023.
- [5] Nathaniel S Keplinger, Baiting Luo, Ilyas Bektas, Yunuo Zhang, Kyle Hollins Wray, Aron Laszka, Abhishek Dubey, and Ayan Mukhopadhyay. Ns-gym: Open-source simulation environments and benchmarks for non-stationary markov decision processes. [arXiv preprint arXiv:2501.09646](#), 2025.
- [6] Jakob Bauer, Kate Baumli, Feryal M. P. Behbahani, Avishkar Bhoopchand, Nathalie Bradley-Schmieg, Michael Chang, Natalie Clay, Adrian Collister, Vibhavari Dasagi, Lucy Gonzalez, Karol Gregor, Edward Hughes, Sheleem Kashem, Maria Loks-Thompson, Hannah Openshaw, Jack Parker-Holder, Shreya Pathak, Nicolas Perez Nieves, Nemanja Rakicevic, Tim Rocktäschel, Yannick Schroecker, Satinder Singh, Jakub Sygnowski, Karl Tuyls, Sarah York, Alexander Zacherl, and Lei M. Zhang. Human-timescale adaptation in an open-ended task space. In Andreas Krause, Emma Brunskill, Kyunghyun Cho, Barbara Engelhardt, Sivan Sabato, and Jonathan Scarlett, editors, [International Conference on Machine Learning, ICML](#), 2023.
- [7] Zhihong Shao, Peiyi Wang, Qihao Zhu, Runxin Xu, Junxiao Song, Xiao Bi, Haowei Zhang, Mingchuan Zhang, YK Li, Yang Wu, et al. Deepseekmath: Pushing the limits of mathematical reasoning in open language models. [arXiv preprint arXiv:2402.03300](#), 2024.
- [8] Yiming Zhang, Yingfan Ma, Yanmei Gu, Zhengkai Yang, Yihong Zhuang, Feng Wang, Zenan Huang, Yuanyuan Wang, Chao Huang, Bowen Song, Cheng Lin, and Junbo Zhao. ABench-Physics: Benchmarking physical reasoning in LLMs via high-difficulty and dynamic physics problems, 2025.
- [9] Daniel J. H. Chung, Zhiqi Gao, Yurii Kvasiuk, Tianyi Li, Moritz Münchmeyer, Maja Rudolph, Frederic Sala, and Sai Chaitanya Tadepalli. Theoretical physics benchmark (TPBench) – a dataset and study of ai reasoning capabilities in theoretical physics, 2025.
- [10] Xinrun Xu, Pi Bu, Ye Wang, Börje F. Karlsson, Ziming Wang, Tengtao Song, Qi Zhu, Jun Song, Zhiming Ding, and Bo Zheng. DeepPHY: Benchmarking agentic VLMs on physical reasoning. [arXiv preprint arXiv:2508.05405](#), 2025.
- [11] Jialong Wu, Shaofeng Yin, Ningya Feng, Xu He, Dong Li, Jianye Hao, and Mingsheng Long. iVideoGPT: Interactive VideoGPTs are scalable world models. [Advances in Neural Information Processing Systems](#), 37:68082–68119, 2024.
- [12] Michael Laskin, Luyu Wang, Junhyuk Oh, Emilio Parisotto, Stephen Spencer, Richie Steigerwald, DJ Strouse, Steven Stenberg Hansen, Angelos Filos, Ethan Brooks, Maxime Gazeau, Himanshu Sahni, Satinder Singh, and Volodymyr Mnih. In-context reinforcement learning with algorithm distillation. In [The Eleventh International Conference on Learning Representations, ICLR](#). OpenReview.net, 2023.
- [13] Volodymyr Mnih, Adrià Puigdomènech Badia, Mehdi Mirza, Alex Graves, Timothy P. Lillicrap, Tim Harley, David Silver, and Koray Kavukcuoglu. Asynchronous methods for deep reinforcement learning. In [Proceedings of the 33rd International Conference on Machine Learning, ICML](#), 2016.
- [14] Ilya Zisman, Vladislav Kurenkov, Alexander Nikulin, Viacheslav Sinii, and Sergey Kolesnikov. Emergence of in-context reinforcement learning from noise distillation. In [Forty-first International Conference on Machine Learning, ICML](#). OpenReview.net, 2024.
- [15] Fahim Tajwar, Yiding Jiang, Abitha Thankaraj, Sumaita Sadia Rahman, J Zico Kolter, Jeff Schneider, and Ruslan Salakhutdinov. Training a generally curious agent. [arXiv preprint arXiv:2502.17543](#), 2025.
- [16] Richard Yuanzhe Pang, Weizhe Yuan, He He, Kyunghyun Cho, Sainbayar Sukhbaatar, and Jason Weston. Iterative reasoning preference optimization. In Amir Globersons, Lester Mackey, Danielle Belgrave, Angela Fan, Ulrich

- Paquet, Jakub M. Tomczak, and Cheng Zhang, editors, Advances in Neural Information Processing Systems 38: Annual Conference on Neural Information Processing Systems 2024, NeurIPS 2024, Vancouver, BC, Canada, December 10 - 15, 2024, 2024.
- [17] Aviral Kumar, Vincent Zhuang, Rishabh Agarwal, Yi Su, John D. Co-Reyes, Avi Singh, Kate Baumli, Shariq Iqbal, Colton Bishop, Rebecca Roelofs, Lei M. Zhang, Kay McKinney, Disha Shrivastava, Cosmin Paduraru, George Tucker, Doina Precup, Feryal M. P. Behbahani, and Aleksandra Faust. Training language models to self-correct via reinforcement learning. In The Thirteenth International Conference on Learning Representations, ICLR. OpenReview.net, 2025.
- [18] Gabriel Sarch, Lawrence Jang, Michael J. Tarr, William W. Cohen, Kenneth Marino, and Katerina Fragkiadaki. VLM agents generate their own memories: Distilling experience into embodied programs of thought. In Advances in Neural Information Processing Systems 38: Annual Conference on Neural Information Processing Systems (NeurIPS), 2024.
- [19] Adam Stooke, Anuj Mahajan, Catarina Barros, Charlie Deck, Jakob Bauer, Jakub Sygnowski, Maja Trebacz, Max Jaderberg, Michael Mathieu, Nat McAleese, Nathalie Bradley-Schmieg, Nathaniel Wong, Nicolas Porcel, Roberta Raileanu, Steph Hughes-Fitt, Valentin Dalibard, and Wojciech Marian Czarnecki. Open-ended learning leads to generally capable agents, 2021.
- [20] Minqi Jiang, Edward Grefenstette, and Tim Rocktäschel. Prioritized level replay. In Proceedings of the 38th International Conference on Machine Learning, ICML, 2021.
- [21] Michael Dennis, Natasha Jaques, Eugene Vinitzky, Alexandre M. Bayen, Stuart Russell, Andrew Critch, and Sergey Levine. Emergent complexity and zero-shot transfer via unsupervised environment design. In Advances in Neural Information Processing Systems 33: Annual Conference on Neural Information Processing Systems, NeurIPS, 2020.
- [22] Minqi Jiang, Michael Dennis, Jack Parker-Holder, Jakob N. Foerster, Edward Grefenstette, and Tim Rocktäschel. Replay-guided adversarial environment design. In Advances in Neural Information Processing Systems 34: Annual Conference on Neural Information Processing Systems, NeurIPS, 2021.
- [23] Jack Parker-Holder, Minqi Jiang, Michael Dennis, Mikayel Samvelyan, Jakob N. Foerster, Edward Grefenstette, and Tim Rocktäschel. Evolving curricula with regret-based environment design. In International Conference on Machine Learning, ICML, 2022.
- [24] Alexander Rutherford, Michael Beukman, Timon Willi, Bruno Lacerda, Nick Hawes, and Jakob N. Foerster. No regrets: Investigating and improving regret approximations for curriculum discovery. In Advances in Neural Information Processing Systems 38: Annual Conference on Neural Information Processing Systems, NeurIPS, 2024.
- [25] Samuel Garcin, James Doran, Shangmin Guo, Christopher G. Lucas, and Stefano V. Albrecht. DRED: zero-shot transfer in reinforcement learning via data-regularised environment design. In Forty-first International Conference on Machine Learning, ICML, 2024.
- [26] Sam Earle and Julian Togelius. Autoverse: An evolvable game language for learning robust embodied agents, 2024.
- [27] Kevin Frans and Phillip Isola. Powderworld: A platform for understanding generalization via rich task distributions. In The Eleventh International Conference on Learning Representations, ICLR, 2023.
- [28] Hao Luo, Jiechuan Jiang, and Zongqing Lu. Model-based decentralized policy optimization. arXiv preprint arXiv:2302.08139, 2023.
- [29] Jieru Lin, Zhiwei Yu, and Börje F. Karlsson. SWITCH: Benchmarking modeling and handling of tangible interfaces in long-horizon embodied scenarios. arXiv preprint arXiv:2511.17649, 2025.
- [30] Haoqi Yuan, Yu Bai, Yuhui Fu, Bohan Zhou, Yicheng Feng, Xinrun Xu, Yi Zhan, Börje F. Karlsson, and Zongqing Lu. Being-0: A Humanoid Robotic Agent with Vision-Language Models and Modular Skills. arXiv preprint arXiv:2503.12533, 2025.
- [31] Wei Chow, Jiageng Mao, Boyi Li, Daniel Seita, Vitor Guizilini, and Yue Wang. Physbench: Benchmarking and enhancing vision-language models for physical world understanding, 2025.

- [32] Lintao Wang, Encheng Su, Jiaqi Liu, Pengze Li, Peng Xia, Jiabei Xiao, Wenlong Zhang, Xinnan Dai, Xi Chen, Yuan Meng, Mingyu Ding, Lei Bai, Wanli Ouyang, Shixiang Tang, Aoran Wang, and Xinzhu Ma. Physunibench: An undergraduate-level physics reasoning benchmark for multimodal models, 2025.
- [33] Anton Bakhtin, Laurens van der Maaten, Justin Johnson, Laura Gustafson, and Ross Girshick. Phyre: A new benchmark for physical reasoning. *Advances in Neural Information Processing Systems, NeurIPS*, 32, 2019.
- [34] Shiqian Li, Kewen Wu, Chi Zhang, and Yixin Zhu. I-PHYRE: interactive physical reasoning. In *The Twelfth International Conference on Learning Representations, ICLR 2024*, 2024.
- [35] Michael T. Matthews, Michael Beukman, Chris Lu, and Jakob Nicolaus Foerster. Kinetix: Investigating the training of general agents through open-ended physics-based control tasks. In *The Thirteenth International Conference on Learning Representations, ICLR 2025*, 2025.
- [36] Anoop Cherian, Radu Corcodel, Siddarth Jain, and Diego Romeres. LLMPhy: Complex physical reasoning using large language models and world models, 2024.
- [37] Weihao Tan, Wentao Zhang, Xinrun Xu, Haochong Xia, Ziluo Ding, Boyu Li, Bohan Zhou, Junpeng Yue, Jiechuan Jiang, Yewen Li, Ruyi An, Molei Qin, Chuqiao Zong, Longtao Zheng, Yujie Wu, Xiaoqiang Chai, Yifei Bi, Tianbao Xie, Pengjie Gu, Xiyun Li, Ceyao Zhang, Long Tian, Chaojie Wang, Xinrun Wang, Börje F. Karlsson, Bo An, Shuicheng Yan, and Zongqing Lu. Cradle: Empowering foundation agents towards general computer control. In *Forty-second International Conference on Machine Learning (ICML)*, 2025.
- [38] Peng Chen, Pi Bu, Yingyao Wang, Xinyi Wang, Ziming Wang, Jie Guo, Yingxiu Zhao, Qi Zhu, Jun Song, Siran Yang, Jiamang Wang, and Bo Zheng. CombatVLA: An efficient vision-language-action model for combat tasks in 3D action role-playing games. In *Proceedings of the IEEE/CVF International Conference on Computer Vision (ICCV)*, 2025.
- [39] Han Qi, Haocheng Yin, Aris Zhu, Yilun Du, and Heng Yang. Strengthening generative robot policies through predictive world modeling. *arXiv preprint arXiv:2502.00622*, 2025.
- [40] Delong Chen, Theo Moutakanni, Willy Chung, Yejin Bang, Ziwei Ji, Allen Bolourchi, and Pascale Fung. Planning with reasoning using vision language world model. *arXiv preprint arXiv:2509.02722*, 2025.
- [41] David Silver, Julian Schrittwieser, Karen Simonyan, Ioannis Antonoglou, Aja Huang, Arthur Guez, Thomas Hubert, Lucas Baker, Matthew Lai, Adrian Bolton, et al. Mastering the game of go without human knowledge. *Nature*, 550(7676):354–359, 2017.
- [42] Kangrui Wang, Pingyue Zhang, Zihan Wang, Yaning Gao, Linjie Li, Qineng Wang, Hanyang Chen, Chi Wan, Yiping Lu, Zhengyuan Yang, Lijuan Wang, Ranjay Krishna, Jiajun Wu, Li Fei-Fei, Yejin Choi, and Manling Li. Reinforcing visual state reasoning for multi-turn VLM agents, 2025.
- [43] Evan Kiefl. Pooltool: A python package for realistic billiards simulation. *Journal of Open Source Software*, 9(101):7301, 2024.
- [44] Qwen Team. Qwen2.5-VL, January 2025.
- [45] Anthropic. System Card: Claude Opus 4 & Claude Sonnet 4, 05 2025. Accessed: 2025-07-01.
- [46] Gheorghe Comanici and et al. Gemini 2.5: Pushing the frontier with advanced reasoning, multimodality, long context, and next generation agentic capabilities, 2025.
- [47] OpenAI. OpenAI o3 and o4-mini System Card, April 2025.
- [48] OpenAI. Gpt-4o system card, 2024.

## Appendix A: Model Abbreviations

The abbreviations used throughout the paper and the full details of the corresponding open-source and closed-source models are listed in Table 7.

Table 7: List of Models Abbreviations

Model	Abbreviation	
<i>MOCK</i>	<i>MOCK</i>	
<b>Open-Source Models</b>		
<b>Qwen2.5-VL Series</b>		
Qwen2.5-VL-3B-Instruct	Qwen-3B	
Qwen2.5-VL-7B-Instruct	Qwen-7B	
Qwen2.5-VL-32B-Instruct	Qwen-32B	
Qwen2.5-VL-72B-Instruct	Qwen-72B	
<b>Closed-Source Models</b>		
Claude 4.0 Opus	[45]	Claude 4.0 Opus
Gemini-2.5-Pro-06-17	[46]	Gemini-2.5-Pro
GPT-o3-0416	[47]	GPT-o3

To clearly distinguish the fine-tuned models developed in our work, we adopt a systematic naming convention, which we illustrate using the Qwen-3B model as example. The names for the Qwen-7B-based models follow the same convention. We use **GREEN** to denote Policy Models and **ORANGE** for World Models.

**Policy Models.** The nomenclature for our Policy Models follows the format:  $\text{BaseModel}^{\text{EnvData-Type}} \text{Method}$ . Each component in the naming structure is defined as follows:

- **Env:** This component begins by indicating the environment(s) used in fine-tuning:
  - **P:** Denotes fine-tuning exclusively on *PHYRE*.
  - **I:** Denotes fine-tuning exclusively on *I-PHYRE*.
  - **P&I:** Denotes a model trained using tasks from both the *PHYRE* and *I-PHYRE* environments.
- **Method:** This term specifies the training algorithm used:
  - **SFT:** Supervised Fine-Tuning.
  - **GRPO:** Group Relative Policy Optimization [7].
- **Data-Type:** An optional subscript for the environment term specifies the nature of the training data:
  - **(No subscript):** The model was trained on a dataset of successful solution trajectories collected from expert models - Gemini-2.5-Pro [46], GPT-4o, and GPT-4o-mini [48]. These trajectories were often generated over multiple attempts (typically 5–10) to find a solution. This strategy is designed to enable the model to learn from a process of trial and error, even within a supervised framework. Our experimental results support this methodology, showing it is consistent with the philosophy of ICRL.
  - **single:** The model was trained on a dataset of first-attempt successful trajectories. These trajectories were generated via a systematic enumeration process over the action space.

For example, the model named **Qwen-3B<sup>P<sub>single</sub> SFT</sup>** is a policy model based on Qwen2.5-VL-3B-Instruct, trained via SFT, only on single-attempt successful trajectories from the *PHYRE* environment.

**World Models.** The naming for our **World Models** is more concise. As all world models are SFT. A given name, such as **Qwen-3B<sup>P</sup>**, directly specifies the base model (Qwen2.5-VL-3B-Instruct) and the environment (*PHYRE*) used for its training.

World models can take one possible subscript: “*w/o 5 Frames*”. This subscript, meaning “without 5 frames,” represents a crucial detail about its training dataset. As described in Subsection 4.3, this particular world model was trained on a curated dataset that *excluded* the five uniformly sampled post-action video frames.